Elimination of spurious kinematic modes in hybrid equilibrium elements

Francesco Parrinello, Guido Borino
Departmento di Ingegneria Civile, Ambientale e Aerospaziale , Universit di Palermo
E-mail: francesco.parrinello@unipa.it, borino@unipa.it

SUMMARY. Hybrid stress elements are proposed as alternative to standard finite elements for linear and non linear analysis. Hybrid stress formulation is developed in a rigorous mathematical setting and an original approach for elimination of spurious kinematic modes is presented. Hybrid equilibrium method is compared to classical displacement based method by linear elastic analysis of some well known structural examples.

1 INTRODUCTION

Finite element formulation based on stress fields satisfying locally equilibrium condition are known in literature since 1964 by the pioneering work of de Vebeuke [1, 2]. Equilibrated elements were initially proposed [3, 4, 5, 6, 7] as numerical tool for error estimation of classical displacement based analyses. In fact equilibrium and displacement formulations produce respectively upper bound and lower bound, with respect to the exact solution, in terms of elastic strain energy. Despite equilibrium formulation has not gained a widespread use, especially in commercial codes, it could be suitable in several fields of computational mechanics, such as: cohesive crack propagation, where accuracy of stress is a fundamental requirement; lower bound limit and shakedown analyses, especially for non-associative rule; topology structural optimization.

Equilibrium elements may be developed in hybrid formulation by use of independent stress fields on each element [8, 9], producing solution which satisfy strong equilibrium condition throughout the domain with co-diffusive traction at each side. In hybrid formulation, traction equilibrium condition, at sides between adjacent elements and at sides of free boundary, is enforced by use of independent displacement laws at each side, assumed as lagrangian parameters.

Hybrid equilibrium formulation is defined by: element stress fields, satisfying homogeneous equilibrium equation and defined as polynomial function; independent displacement polynomial laws at each sides. Strong traction equilibrium condition require the same interpolation order for stress and displacement fields, which can produces Spurious Kinematic Modes (SKMs), that are displacement modes with null traction at sides. SKMs can heavily corrupt the elastic solution both in terms of displacement and in terms of stress. In some patch of mesh, SKMs do not propagate and remain confined inside the group of elements. Such a condition has inspired several approaches [9, 10, 11, 12], able to control or eliminate SKMs, which use the super-element obtained by assembling the group of elements in which SKM is confined inside. The super-element is connected to the other elements through its external sides, whereas the degrees of freedom of internal sides are condensed out. The condensation procedure, that must be performed for many super-elements, could require a considerable computational cost.

The analysis of possible SKM in a patch of elements can be performed by the algebraic procedure proposed by [13], evaluating the rank of a rectangular compatibility matrix. The present paper proposes an alternative approach for elimination of SKMs in some patches of mesh, well known in literature. Due to the fact that SKMs are associated to the rank deficiency in the global stiffness

matrix, detection of linearly dependent equations is the first step for SKM elimination. Then, the algebraic equation system is reduced to a full rank one by elimination of the dependent equations, for which the resolution strategies is based on the use of a kinematic constrain between degrees of freedom involved in the dependent equations. The proposed procedure does not require any additional computational cost; on the contrary, it reduce the overall equation system.

In the present paper, the dependent equations are detected by analysis of side equilibrium equations of three specific patches of elements. The latter analysis can not be easily generalized for generic meshes.

2 Minimum complementary energy principle

Let an elastic body of volume Ω be considered on a two dimensional Cartesian reference (x, y), subjected to body force b_i in Ω, traction t_i on the free boundary Γ_t and imposed displacement $\overline{u}_i$ on the constrained boundary $\Gamma_u = \Gamma - \Gamma_t$.

The elastostatic response, in terms of stress σ_{ij}, strain ϵ_{ij} and displacement u_i can be obtained: in strong form, as solution of governing partial differential equations; in weak form, as stationary condition of a integral functional. The weak equilibrium approach is based on the following total complementary energy functional

$$\Pi_c = \frac{1}{2} \int_\Omega \sigma_{ij} \, D_{ijhk} \, \sigma_{hk} \, d\Omega - \int_{\Gamma_u} \sigma_{ij} \, n_j \, \overline{u}_i \, d\Gamma \tag{1}$$

where stress field σ_{ij} is assumed to satisfy domain and boundary equilibrium equations

$$\frac{\partial \sigma_{ij}}{\partial x_j} + b_i = 0 \ \ in \ \Omega \tag{2}$$

$$\sigma_{ij} \, n_j = t_i \ \ on \ \Gamma_t. \tag{3}$$

Functional Π_c is defined in the space of all statically admissible solutions (stress fields satisfying eq. (2) and eq. (3)) and, in such space, the point where Π_c is stationary characterize the stress field solution of the elastostatic problem.

Equilibrium element is defined by statically admissible internal stress fields $\sigma_{ij}^{(e)}$ in its domain Ω_e, which must verify inter-element equilibrium, condition, at all internal sides $\Gamma_s \subset \partial\Omega_e - \Gamma_t$, and boundary equilibrium condition on all free boundary sides $\Gamma_s \subset \partial\Omega_e \cap \Gamma_t$. The latter two conditions can be properly applied by following the classical hybrid formulation. Independent lagrangian displacements v_i, defined on each the element side, are used to mutually connect adjacent elements and to apply traction on the free boundary. For a triangular finite element discretization, the weak form of lagrangian approach gives the following modified total complementary energy functional

$$\overline{\Pi}_c = \sum_{e=1}^{Ne} \left[\frac{1}{2} \int_{\Omega_e} \sigma_{ij}^{(e)} \, D_{ijhk} \, \sigma_{hk}^{(e)} \, d\Omega - \sum_{s=1}^{3} \int_{\Gamma_s \subset \partial\Omega_e} \sigma_{ij}^{(e)} \, n_j \, v_i \, d\Gamma \right] + \int_{\Gamma_s \subset \Gamma_t} t_i \, v_i \, d\Gamma \tag{4}$$

with $v_i = \overline{u}_i$ on $\Gamma_s \subset \Gamma_u$. In eq. (4) n_j represents the outward normal to side $\Gamma_s \subset \partial\Omega_e$.

Stationary conditions of functional $\overline{\Pi}_c$, with respect to the lagrangian variable v_i of the internal side $\Gamma_s = \partial\Omega_{e_1} \cap \partial\Omega_{e_2}$ between elements e_1 and e_2, gives

$$-\int_{\Gamma_s} \left(\sigma_{ij}^{(e_1)} \, n_j^{(e_1)} + \sigma_{ij}^{(e_2)} \, n_j^{(e_2)} \right) \delta v_i \, d\Gamma = 0 \tag{5}$$

where, outward normals are $n_j^{(e_1)} = -n_j^{(e_2)}$. For a free boundary side $\Gamma_s = \partial\Omega_e \cap \Gamma_t$ stationary condition gives

$$-\int_{\Gamma_s} \left(\sigma_{ij}^{(e)} \, n_j^{(e)} - t_i \right) \delta v_i \, d\Gamma = 0. \tag{6}$$

Equations (5) and (6) provide weak form of inter-element and boundary equilibrium conditions.

3 Hybrid equilibrium element

The equilibrium approach of elastostatic problem by finite element method is based on minimization of functional $\overline{\Pi}_c$ in eq. (4) and involve hybrid formulation. Each finite element is defined by internal stress field satisfying domain equilibrium equation (3), which does not interpolate nodal degree of freedom, but is function of internal generalized stresses. Independent side displacements are used as interface Lagrangian variable linking the two adjacent elements, for internal sides, or linking the element side traction to the external load, for the free boundary sides. In the present paper, hybrid equilibrium element is developed only for two dimensional membrane elastostatic problems; implementation and numerical results are proposed only for triangular finite elements with quadratic stress field.

Let a triangular finite element of domain Ω_e be considered with straight sides, referred to a local Cartesian reference (x, y), which is parallel to the global one (X, Y), but centered at vertex 1. The membrane stress fields are defined by the following quadratic polynomial functions

$$\sigma_x = a_1 + a_2 x + a_3 y + 2a_4 xy + a_5 x^2 + a_6 y^2 - b_x x \tag{7}$$

$$\sigma_y = a_7 + a_8 x + a_9 y + 2a_{10} xy + a_{11} x^2 + a_5 y^2 - b_y y \tag{8}$$

$$\tau_{xy} = a_{12} - a_9 x - a_2 y - 2a_5 xy - a_{10} x^2 - a_4 y^2 \tag{9}$$

where, b_x and b_y are components of body force, and terms $a_1, \ldots, a_{12}$ are generalized stress variables. Stress field of eq. (7-9) implicitly satisfies equilibrium equation (2) and can be represented in the following matrix notation

$$\boldsymbol{\sigma} = \mathbf{S} \cdot \mathbf{a} + \boldsymbol{\sigma}_0 \tag{10}$$

where $\mathbf{a}$ collects all generalized stress and $\boldsymbol{\sigma}_0 = [-b_x x, -b_y y, 0]^T$ is a particular solution of eq. (2) for the body load presence.

Normal and tangential side displacements are defined in the following form

$$\overline{v}_t(\xi) = N_i(\xi) u_i^t \tag{11}$$

$$\overline{v}_n(\xi) = N_i(\xi) u_i^n \tag{12}$$

where: $N_i(\xi)$ is the ith shape function in natural coordinate $-1 \leq \xi \leq 1$, u_i^t and u_i^n are the relevant kinematic degrees of freedom. In matrix notation, eqs.(11, 12) are rewritten as

$$\overline{\mathbf{v}} = \mathbf{N} \cdot \mathbf{u}, \tag{13}$$

where, $\mathbf{N}$ collects the shape functions and $\mathbf{u}$ collects the side kinematic degrees of freedom.

For an elastostatic problem with null body force, whose domain is discretized in n_e triangular finite elements and whose free boundary is divided in n_s element sides, the the complementary energy functional $\overline{\Pi}_c$ is

$$\overline{\Pi}_c = \sum_{e=1}^{n_e} \left[\frac{1}{2} \mathbf{a}_e^T \mathbf{k}_e^{aa} \mathbf{a}_e - \sum_{s=1}^{3} \mathbf{a}_e^T \mathbf{k}_{e,s}^{au} \mathbf{u}_s \right] + \sum_{s=1}^{n_s} \mathbf{T}_s^T \mathbf{u}_s \tag{14}$$

where

$$\mathbf{k}_e^{aa} = \int_{\Omega_e} \mathbf{S}_e^T \mathbf{D} \mathbf{S}_e d\Omega \tag{15}$$

$$\mathbf{k}_{e,s}^{au} = \int_{\Gamma_s} \mathbf{S}_e^T \mathbf{h}_{e,s} \, \mathbf{g}_s \mathbf{N} d\Gamma \tag{16}$$

$$\mathbf{T}_s^T = \int_{\Gamma_s} \mathbf{t}^T \mathbf{g}_s \mathbf{N} d\Gamma \tag{17}$$

$$\mathbf{h}_{e,s} = \pm \begin{bmatrix} n_{sx} & 0 \\ 0 & n_{sy} \\ n_{sy} & n_{sx} \end{bmatrix} \tag{18}$$

where the sign in the latter equation is positive if axes $\mathbf{n}_s$ is outward from element. The degrees of freedom of side lying on the constrained boundary Γ_u are constrained, with assigned value $\overline{\mathbf{u}}$. Algebraic solving equations of the hybrid equilibrium formulation are defined as stationary conditions of functional $\overline{\overline{\Pi}}_c$ in eq. (14), that are

$$\frac{\partial \overline{\overline{\Pi}}_c}{\partial \mathbf{a}_e} = \mathbf{k}_e^{aa} \mathbf{a}_e - \mathbf{k}_{e,s_1}^{au} \mathbf{u}_{s_1} - \mathbf{k}_{e,s_2}^{au} \mathbf{u}_{s_2} - \mathbf{k}_{e,s_3}^{au} \mathbf{u}_{s_3} = 0 \tag{19}$$

$$\frac{\partial \overline{\overline{\Pi}}_c}{\partial \mathbf{u}_s} = -\mathbf{k}_{e1,s}^{au}{}^T \mathbf{a}_{e_1} - \mathbf{k}_{e2,s}^{au}{}^T \mathbf{a}_{e_2} = 0 \quad \text{for } \Gamma_s = \partial \Omega_{e1} \cap \Omega_{e2} \tag{20}$$

$$\frac{\partial \overline{\overline{\Pi}}_c}{\partial \mathbf{u}_s} = -\mathbf{k}_{e,s}^{au}{}^T \mathbf{a}_e + \mathbf{T}_s = 0 \quad \text{for } \Gamma_s = \partial \Omega_e \cap \Gamma_t. \tag{21}$$

with s_1, s_2 and s_3 sides of element e. After assembling operations, the following system of algebraic equations is obtained

$$\begin{bmatrix} \mathbf{K}_{AA} & -\mathbf{K}_{AU} \\ -\mathbf{K}_{UA} & \mathbf{0} \end{bmatrix} \begin{bmatrix} \mathbf{A} \\ \mathbf{U} \end{bmatrix} = \begin{bmatrix} \mathbf{0} \\ -\mathbf{T} \end{bmatrix} \tag{22}$$

where vector $\mathbf{A}$ collects all generalized stress variables and vector $\mathbf{U}$ collects kinematic degrees of freedom of all sides. Moreover, matrix $\mathbf{K}_{AA}$ is composed of diagonal blocks $\mathbf{K}_e^{aa}$, each of which is symmetric, positive definite and not singular, so that $\mathbf{K}_{AA}$ can be inverted and the relevant degrees of freedom $\mathbf{A}$ can be condensed out and the solving equations system can be defined only in function of side displacements

$$\mathbf{K}_{UU} \mathbf{U} = \mathbf{T}, \tag{23}$$

which can be solved as in a standard finite element approach.

4   Spurious kinematic modes

In this section, the geometrical conditions of some patch of elements, under which Spurious kinematic Modes (SKMs) emerge, are investigated. The SKM (or zero energy mode) is a set of side displacement which produces null stress field and, consequently, null side traction. The presence of SKMs is analyzed for a single element and for two stars of elements, which are well known in literature [13] for the emerging SKMs: namely, the open star of two adjacent elements on the free boundary and the closed star of four element. In [13], the presence of SKMs is predicted as a function of the rank of a compatibility matrix, which is constructed by assembling SMKs of each single element of the star.

Presence of SKMs is associated to the rank deficiency in the global stiffness matrix $\mathbf{K}_{UU}$ of eq.(23), which is produced by one or more linearly dependent equations in the set of inter-element equilibrium equations (20) and boundary equilibrium equations (21). For a boundary side $\Gamma_s = \partial\Omega_e \cap \Gamma_t$, applied tractions $\mathbf{t}_s(\xi)$ can be defined in the following interpolation form

$$\mathbf{t}_s(\xi) = \mathbf{g}_s \mathbf{N}(\xi) \mathbf{f}_s \tag{24}$$

where $\mathbf{N}(\xi)$ is the matrix of shape functions, $\mathbf{f}_s$ is a vector collecting normal and tangential traction components at interpolation points $\mathbf{x}_{s,i}$, as shown in Fig. 1a. Moreover, strongly enforcement of boundary equilibrium equation (3) is assured by using the same order of stress field $\boldsymbol{\sigma}(\mathbf{x}) = \mathbf{S}(\mathbf{x})\,\mathbf{a}$ and of displacement law $\bar{\mathbf{v}} = \mathbf{N} \cdot \mathbf{u}$. Than, solution of eq.(21) is given by

$$\begin{bmatrix} n_{sx}n_{sy} & -n_{sx}n_{sy} & n_{sy}^2 - n_{sx}^2 \end{bmatrix} \mathbf{S}_e(\mathbf{x}_{s,j})\mathbf{a} = f_{s,j}^t \tag{25}$$

$$\begin{bmatrix} n_{sx}^2 & n_{sy}^2 & 2n_{sy}n_{sx} \end{bmatrix} \mathbf{S}_e(\mathbf{x}_{s,j})\mathbf{a} = f_{s,j}^n, \tag{26}$$

which ensure that internal stress field strongly verifies boundary equilibrium conditions (3) at the three interpolation points and, consequently, at the entire side Γ_s. Equations (25) and (26) can be written in the following simplified form

$$\tau_e(\mathbf{x}_{s,j}) = f_{s,j}^t \tag{27}$$

$$\sigma_e(\mathbf{x}_{s,j}) = f_{s,j}^n, \tag{28}$$

where $\tau_e(\mathbf{x}_{s,j})$ and $\sigma_e(\mathbf{x}_{s,j})$ are respectively tangential and normal stress components at j^{th} interpolation point of boundary side Γ_s.

For an internal side $\Gamma_s = \partial\Omega_{e1} \cap \partial\Omega_{e2}$, considering the same interpolation order for the two elements stress fields and for the the side displacement law, the solution of inter-element equilibrium equation (20) is

$$\begin{bmatrix} n_{sx}n_{sy} & -n_{sx}n_{sy} & n_{sy}^2 - n_{sx}^2 \end{bmatrix} \mathbf{S}_{e_1}(\mathbf{x}_{s,j}^{e_1})\mathbf{a}_{e_1} = \begin{bmatrix} n_{sx}n_{sy} & -n_{sx}n_{sy} & n_{sy}^2 - n_{sx}^2 \end{bmatrix} \mathbf{S}_{e_2}(\mathbf{x}_{s,j}^{e_2})\mathbf{a}_{e_2} \tag{29}$$

$$\begin{bmatrix} n_{sx}^2 & n_{sy}^2 & 2n_{sy}n_{sx} \end{bmatrix} \mathbf{S}_{e_1}(\mathbf{x}_{s,j}^{e_1})\mathbf{a}_{e_1} = \begin{bmatrix} n_{sx}^2 & n_{sy}^2 & 2n_{sy}n_{sx} \end{bmatrix} \mathbf{S}_{e_2}(\mathbf{x}_{s,j}^{e_2})\mathbf{a}_{e_2}, \tag{30}$$

or in simplified form

$$\tau_{e_1}(\mathbf{x}_{s,j}) = \tau_{e_2}(\mathbf{x}_{s,j}) \tag{31}$$

$$\sigma_{e_1}(\mathbf{x}_{s,j}) = \sigma_{e_2}(\mathbf{x}_{s,j}), \tag{32}$$

which ensure that internal stress fields in elements e_1 and e_2 are co-diffusive at the three interpolating points and, consequently, along the entire side.

4.1 SKM in a single element

A single triangular equilibrium element with quadratic stress field is defined by $n_s = 12$ stress parameters (dimension of vector $\mathbf{a}$) and by $3\,n_v = 18$ displacement degrees of freedom (n_v is the dimension of vector $\mathbf{u}_s$). With reference to eq.(23), the global stiffness matrix of the single element, without constrained sides, can be written as

$$\mathbf{K}_{UU} = \begin{bmatrix} \mathbf{k}_1^{auT} & \mathbf{k}_2^{auT} & \mathbf{k}_3^{auT} \end{bmatrix} \mathbf{k}_e^{aa-1} \begin{bmatrix} \mathbf{k}_1^{au} \\ \mathbf{k}_2^{au} \\ \mathbf{k}_3^{au} \end{bmatrix} \tag{33}$$
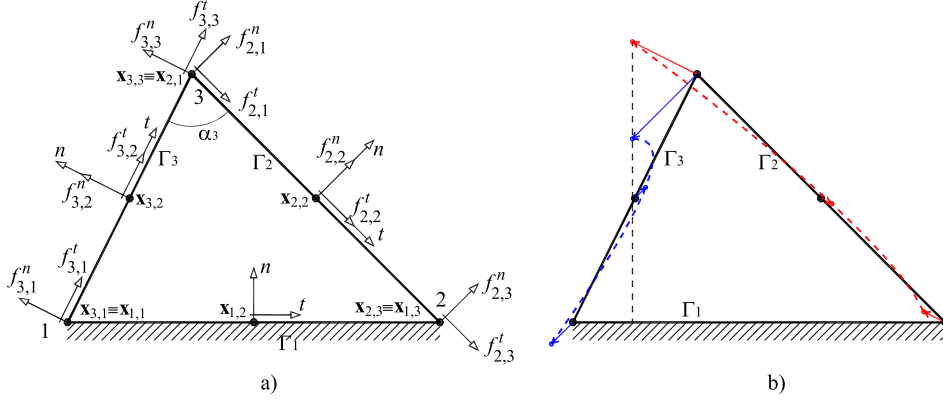
5

Figure 1: a) Constrained triangular element; b) SKM on constrained element

where it can be observed that rank r_K of matrix $\mathbf{K}_{UU}$ can not be grater then rank r_a of matrix $\mathbf{k}^{aa}$, than it is $r_K = r_a = 12$. The number of SKM is given as difference between dimension ($n_K = 18$) and rank r_K of matrix $\mathbf{K}_{UU}$; but, in unconstrained structure, three of such modes are due to rigid body motions ($n_{RB} = 3$). Than, the number of SKM is

$$n_{SK} = n_K - r_K - n_{RB} = 3. \tag{34}$$

One SKM is still active in the single element, even if one side is constrained ($s = 1$ in Fig. 1a). Dimension of matrix $\mathbf{K}_{UU}$ is equal to the number of active kinematic variables ($n_K = 12$), all rigid body motion are blocked but, despite it is $n_K = n_s$, stiffness matrix $\mathbf{K}_{UU}$ is not with full rank and it results $r_K = 11$ and $n_{SK} = n_K - r_K = 1$. Side displacements of the emerging SKM, shown initially in [14], are plotted in Fig. 1b where it can be observed that displacement at side Γ_2 is orthogonal to side Γ_3 and *viceversa*.

Reasons of SKM presence can be found by deep analysis of the boundary equilibrium equations (25) and (26) for the two unconstrained sides. Twelve scalar equilibrium equations are obtained and, between them, the following four equations are related to the common corner $\mathbf{x}_3 \equiv \mathbf{x}_{2,1} \equiv \mathbf{x}_{3,3}$

$$\left[n_{2x}n_{2y} \quad -n_{2x}n_{2y} \quad n_{2y}^2 - n_{2x}^2 \right] \mathbf{S}_e(\mathbf{x}_{2,1})\mathbf{a} = \tau_e(\mathbf{x}_{2,1}) = f_{2,1}^t \tag{35}$$

$$\left[n_{2x}^2 \quad n_{2y}^2 \quad 2n_{2y}n_{2x} \right] \mathbf{S}_e(\mathbf{x}_{2,1})\mathbf{a} = \sigma_e(\mathbf{x}_{2,1}) = f_{2,1}^n \tag{36}$$

$$\left[n_{3x}n_{3y} \quad -n_{3x}n_{3y} \quad n_{3y}^2 - n_{3x}^2 \right] \mathbf{S}_e(\mathbf{x}_{3,3})\mathbf{a} = \tau_e(\mathbf{x}_{3,3}) = f_{3,3}^t \tag{37}$$

$$\left[n_{3x}^2 \quad n_{3y}^2 \quad 2n_{3y}n_{3x} \right] \mathbf{S}_e(\mathbf{x}_{3,3})\mathbf{a} = \sigma_e(\mathbf{x}_{3,3}) = f_{3,3}^n \tag{38}$$

The latter equations impose four conditions for the stress tensor $\boldsymbol{\sigma}(\mathbf{x}_3) = \mathbf{S}(\mathbf{x}_3)\,\mathbf{a}$ at the corner $\mathbf{x}_3$, which is defined by only three independent components in planar membrane problems. In fact, for a vertex with orthogonal sides, as in Fig. 2a, the tangential components must be equal $\tau_\xi = \tau_\eta$. More generally, the rotational equilibrium condition of an infinitesimal surface element with non-orthogonal sides, as represented in Fig. 2b, gives

$$\tau_\xi - \tau_\eta = (\sigma_\xi - \sigma_\eta)\cot(\alpha) \tag{39}$$

and for the corner $\mathbf{x}_3$ the last condition is

$$f_{3,3}^t + f_{2,1}^t = \left[f_{3,3}^n - f_{2,1}^n \right]\cot(\alpha_3) \tag{40}$$

which proves that one of the four scalar equations (35-38) linearly depends on each others, causing rank deficiency in the stiffness matrix and the relevant SKM. Moreover, the components of external load at corner must verify eq.(40), otherwise equilibrium can not be achieved.
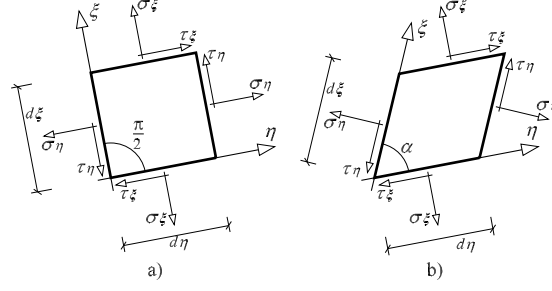
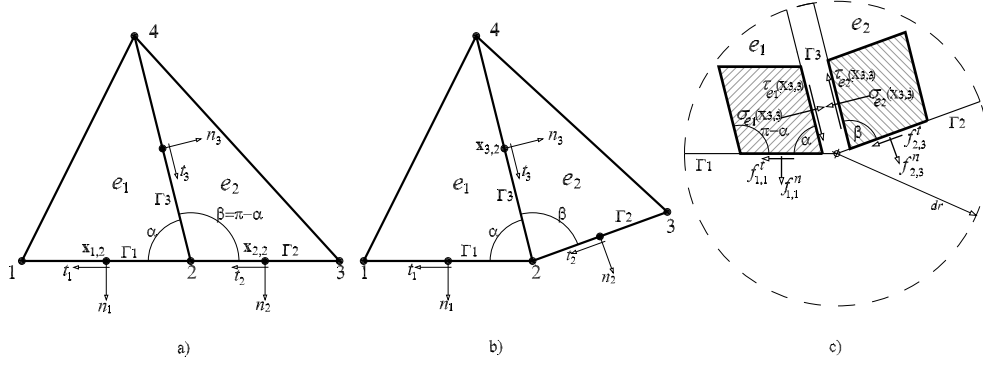Figure 2: Stress components at: a)right angle; b)general angle

Figure 3: a) Open star with parallel boundary sides; b) open star with not parallel boundary sides; c) traction components at the common vertex

4.2 SKMs in an open star of two elements

The open star of elements is a set of two adjacent elements with one boundary side each, as shown in figures (3a, b). Such patch of elements with parallel boundary sides (Fig. 3) presents one SKM. Whereas, the same patch of elements, but with not parallel boundary sides, does not exhibit any SKM. As in previous section (4.1), causes of the emerging SKM can be found by analysis of eqs.(25) and (26) for the two boundary sides, and eqs. (29) and (30) for the common internal side. In particular, at the common vertex 2, represented in Fig. 3c with the relevant traction components and external load components, and considering also the corner equilibrium equation (39) applied to the two adjacent elements, the following relation is obtained

$$\sigma_{e_1}\left(\mathbf{x}_{3,3}\right)\left[\cot\left(\alpha\right)+\cot\left(\beta\right)\right]=f_{1,1}^t-f_{2,3}^t+f_{2,3}^n\cot\left(\beta\right)+f_{1,1}^n\cot\left(\alpha\right), \tag{41}$$

which states that, when boundary sides are not parallel, inter-element normal traction component $\sigma_{e_1}\left(\mathbf{x}_{3,3}\right)$ is function of the external load components; whereas, when boundary sides are parallel $(\beta=\pi-\alpha,\ \cot\left(\beta\right)=-\cot\left(\alpha\right))$, eq.(41) states that one of the four load components depends on the others and, consequently, one of the equilibrium equations linearly depends on the others. Moreover, due to the fact that for parallel boundary sides eq.(41) involves only the external load, such condition must be imposed at the boundary condition level, otherwise equilibrium can not be achieved. Equation (41) involves all the external load components, but if internal side is orthogonal to the two boundary sides $(\alpha=\beta=\pi/2)$, only tangential components are involved.

4.3 SKMs in a closed star of four elements

The closed star of four elements is a set of four elements with an internal common vertex, as shown in figures (4a, b). Two different cases has to be distinguished: the first one, shown in Fig. 4a, where the internal point lies at the diagonals intersection and which present one SKM; the second one, shown in Fig. 4b with the internal point in an other position, which does not present any SKM.
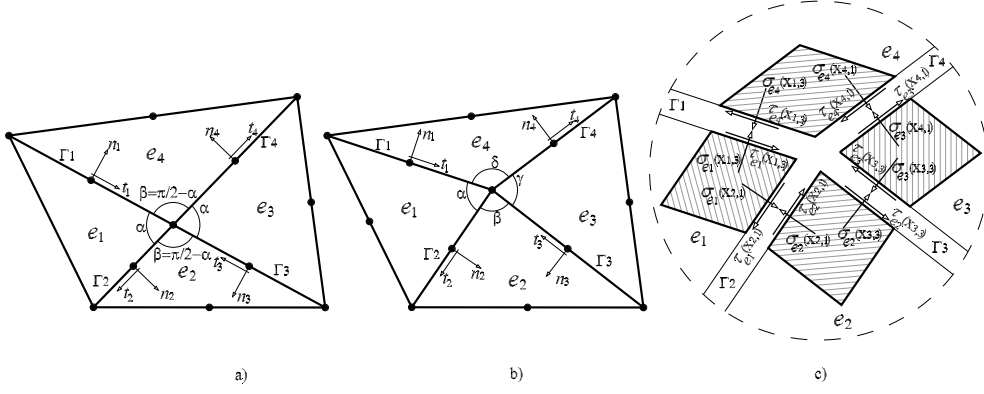
7

Figure 4: a) Closed star with diagonal internal sides; b) closed star with not diagonal internal sides; c) traction components at the internal common vertex

The presence of the SKM when the interior point lies at diagonal intersection is caused by the lost of linear independency in the set of equilibrium equations (29) and (30), for the four internal sides at the internal vertex, and the four equilibrium equations obtained by applying eq.(39) to the corners around internal vertex. Manipulation of such equations gives the following relations

$$\tau_{e_4}\left(\mathbf{x}_{1,3}\right) - \tau_{e_3}\left(\mathbf{x}_{3,3}\right) = -\sigma_{e_1}\left(\mathbf{x}_{4,1}\right)\left[\cot\left(\alpha\right) + \cot\left(\beta\right)\right] + \\ + \sigma_{e_4}\left(\mathbf{x}_{1,3}\right)\cot\left(\alpha\right) + \sigma_{e_3}\left(\mathbf{x}_{3,3}\right)\cot\left(\beta\right) \tag{42}$$

$$\tau_{e_4}\left(\mathbf{x}_{1,3}\right) - \tau_{e_3}\left(\mathbf{x}_{3,3}\right) = +\sigma_{e_1}\left(\mathbf{x}_{2,1}\right)\left[\cot\left(\gamma\right) + \cot\left(\delta\right)\right] + \\ - \sigma_{e_4}\left(\mathbf{x}_{1,3}\right)\cot\left(\delta\right) - \sigma_{e_3}\left(\mathbf{x}_{3,3}\right)\cot\left(\gamma\right), \tag{43}$$

which are mutually independent, but if internal point lies at the diagonals intersection the following conditions hold

$$\cot\left(\alpha\right) = -\cot\left(\beta\right) = \cot\left(\gamma\right) = -\cot\left(\delta\right) \tag{44}$$

and eqs.(42) and (43) become identical, proving that the equilibrium equations are not linearly independent and, as a consequence, the rank of stiffness matrix is not full and one SKM reveals. As in the case of the open star of element, if internal sides are orthogonal ($\alpha = \beta = \gamma = \delta = \pi/2$), dependent equations (42) and (43) only involves tangential components.

5   Restraint of spurious kinematic modes

The proposed approach is based on the elimination of the linearly dependent equations in order to reduce the set of equilibrium equations up to a full rank one. The equation elimination can be performed by constraining the relevant kinematic variable by the master-slave elimination method. Because in some cases linear dependent equations do not involve normal traction components, the constrained variable is always a tangential displacement component.

5.1   Single element

With reference to the problem of SKM in a single element with two boundary sides analyzed in section 4.1, the tangential displacement $u_{3,3}^t$ of side Γ_3 is defined as function of displacement components of the same point $\mathbf{x}_{2,1}$ of side Γ_2 (see Fig. 1a), that is

$$u_{3,3}^t = u_{2,1}^t \cos\left(\alpha_{23}\right) + u_{2,1}^n \sin\left(\alpha_{23}\right) \tag{45}$$

where α_{23} is the angle between the two oriented sides Γ_2 and Γ_3. It can be easily proven that, after application of kinematic restrain of eq.(45), the eleven equilibrium conditions, obtained as stationary conditions with respects to all the independent kinematic variables, and the corner equilibrium

8

equation (40) are a set of twelve coupled and linearly independent equations, whose solution is

$$\tau_e\left(\mathbf{x}_{3,i}\right) = f_{3,i}^t, \ \ \sigma_e\left(\mathbf{x}_{3,i}\right) = f_{3,i}^n, \ \ \tau_e\left(\mathbf{x}_{2,i}\right) = f_{2,i}^t, \ \ \sigma_e\left(\mathbf{x}_{2,i}\right) = f_{2,i}^n, \ \ i = 1, 2, 3 \qquad (46)$$

which impose the boundary conditions at each interpolation point of the boundary sides, and which do not produce any SKM. Therefore, application of kinematic constrain of eq. 45 preserves verified boundary equilibrium equations and it restrains the SKM.

5.2 Open star of two elements

In order to constrain the SKM in the open star of two element with parallel boundary sides shown in Fig. 3a, the kinematic constrain can be applied between tangential degrees of freedom of the common point between sides Γ_1 and Γ_2, that is

$$u_{2,3}^t = u_{1,1}^t, \qquad (47)$$

which is verified in the exact solution.

As in previous case, the stationary conditions produce a set of eleven coupled boundary equilibrium equations for sides Γ_1 and Γ_2 and a set of six uncoupled inter-element equations equations for the internal side Γ_3.

It can be easily proven that application of kinematic constrain of eq.(47) restrains the SKM and it preserves strongly verified both the boundary equilibrium conditions at sides Γ_1 and Γ_2 and the inter-element equilibrium condition at side Γ_3.

5.3 Closed star of four elements

Finally, in order to constrain the SKM in the closed star of four elements with diagonal internal sides, master-slave condition can be applied between two parallel sides, for example between sides Γ_1 and Γ_3 or between sides Γ_2 and Γ_4 (see Fig. 4a). The former case is considered and the relevant kinematic constrain is

$$u_{1,3}^t = -u_{3,3}^t. \qquad (48)$$

where sign minus is due to the opposite verses of local tangential axes of sides Γ_1 and Γ_3. Application of the kinematic constrain of eq.(48) modifies the stationarity conditions of the involved sides and a set of eleven coupled equilibrium equations is obtained. As in the two previous cases, the solutions of such coupled equations, unitedly to the corner equilibrium equation (39) applied to the four corner around the internal vertex and unitedly to the equilibrium equation of sides Γ_2 and Γ_4, strongly keeps verified the co-diffusivity conditions at all internal sides and it restrains the SKM.

6 Numerical results

The hybrid equilibrium element and the proposed restraining approach have been implemented in a specific finite element code for the elastostatic analysis of simple structures. The cantilever beam problem proposed by Cook in [15] is considered in order to verify the proposed restraining approach and in order to compare the solution of hybrid equilibrium approach with the reference one. The beam geometry is represented in Figs. 5a,b with the two load conditions and the two different considered meshes, which are defined by number of node, number and local reference of sides and number of elements. Connectivity information can be easily deduced. Material is isotropic elastic with parameter Young module $E = 1500$, Poisson ratio $\nu = 0.25$ and thickness $h = 1$. The cantilever beam is clamped at the left end, where section deformation is allowed in its self plane,
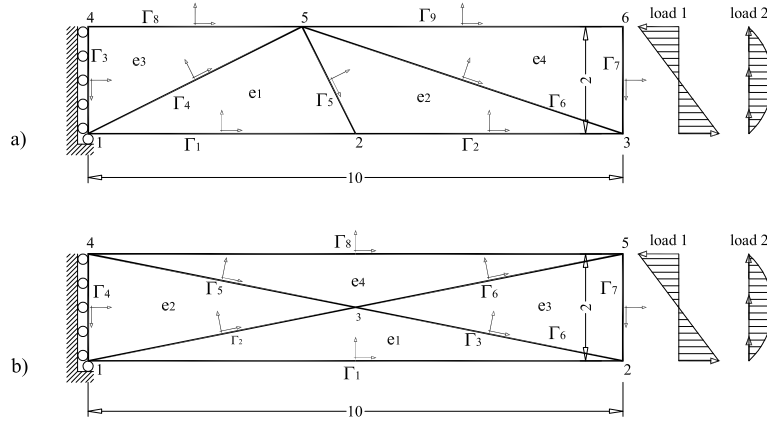
Figure 5: Hybrid equilibrium meshes of the cantilever beam: a) mesh 1; b) mesh 2

and it is loaded at the right end. The same meshes are adopted also for the standard finite element analysis with six-nodes triangular elements (T6).

The load conditions are usually defined as nodal forces, whereas in equilibrium contest they are defined in terms of traction components at the interpolation points. Load one is usually defined by a couple of nodal force $Fx = \pm 1000$ applied at the corner but, in the present approach, it is applied as a linear distribution of normal stress, as shown in Figs. 5a,b. Load two is usually defined by a tangential force $Fy = \pm 300$ but it is applied by a quadratic distribution of tangential stresses, which vanish at the corners. In fact, due to the fact that the two horizontal external surfaces are unloaded and in order to impose rotational equilibrium equation 39, tangential stress at the two corners of the vertical right side must be null.

The considered meshes present some SKMs which must be restrained, otherwise numerical analysis cannot be performed. In details, mesh one (Fig. 5a) presents three SKMs: the first one is due by the open star with parallel boundary sides of elements e_1 and e_2; the second and the third one are respectively caused by element e_3 and by element e_4 because they present two boundary sides each. Mesh two (Fig. 5b) presents one SKM because the mesh is a closed star of four element where internal point lies at diagonal intersection. Such remarks are confirmed by the eigenvalue analysis of the global stiffness matrix of the two different discretizations. Some significant eigenvalues of the two meshes, with and without application of the restraining approach (RA), are report in the following table 1. The relevant eigenvalues are compared in table 1 with eigenvalues of the original problems and, in both cases, the absence of null eigenvalue confirm that all the SKMs are restrained by the proposed approach.

The elastostatic response of the cantilever beam subjected to load 1, obtained with both the two meshes by the hybrid equilibrium method and by application of the proposed restraining approach, coincides with exact solution both in terms of stresses and in terms of sides displacement. In fact, in exact solution stresses are constant in the horizontal direction and are linear in the vertical one therefore, such solution can be properly reproduced by the proposed quadratic elements, independently by the adopted mesh. Exact solution is obtained also with displacement T6 elements.

The elastostatic responses of the cantilever beam subjected to load 2 does not coincide with exact solution. The results are compared with the reference solutions [15] in table 2 in terms of vertical displacement of the lower-right corner, for all sides containing such point. It can be observed that

	Mesh 1		Mesh 1+RA		Mesh 2		Mesh 2+RA
nr	Eigenvalue	nr	Eigenvalue	nr	Eigenvalue	nr	Eigenvalue
1	47613.86	1	47673.9	1	75418.25	1	75328.63
2	32324.52	2	32306.03	2	65882.18	2	65893.61
3	22369.74	3	22325.38	3	53124.1	3	53264.35
4	19864.39	4	19769.43	4	37102.99	4	37036.28
$\vdots$	$\vdots$	$\vdots$	$\vdots$	$\vdots$	$\vdots$	$\vdots$	$\vdots$
46	1.42	46	1.33	40	11.25	40	11.32
47	0.71	47	0.5	41	3.09	41	3.09
48	3.47E-07			42	1.44	42	1.44
49	-1.18E-07			43	0.26	43	0.26
50	-4.00E-08			44	-3.02E-06		

Table 1: Eigenvalues of mesh one and mesh two with and without restraining approach (RA)

	Mesh 1+RA			Mesh 2+RA			T6		
	Γ_2	Γ_6	Γ_7	Γ_1	Γ_3	Γ_6	mesh 1	mesh 2	**Ref.[15]**
u_y	103.03	103.28	102.80	105.2	102.92	102.7	96.8	85	**102.6**
error %	0.42	0.66	0.19	2.53	0.31	0.10	-5.74	-17.2	

Table 2: Load 2 vertical displacement of the lower-right corner

displacements of different sides, at the same point, are not equal and the compatibility condition is not verified. Nevertheless, except side 1 of mesh 2, the error is less than 1%, which is very small for the coarse meshes adopted. The deformed configuration of the two meshes subjected to load 2 are represented in Figs. 6a,b, with displacement factor equal to 0.015.

Table 2 reports also the numerical solution of classical displacement based approach (T6), which produces much higher error than hybrid equilibrium approach, despite based on the same discretization.

7 Conclusions

Hybrid equilibrium elements represent an important numerical tool for the structural analysis, but its use is strongly discouraged because the presence of potential spurious kinematic modes (SKM) can not be easily predicted. In the present paper, causes of the emerging SKM are investigated for three different patches of elements, well known in literature for the presence of SKM. Geometrical conditions under which SKMs reveal and the relevant mathematical motivation are determined, unitedly to the set of linear dependent equations producing rank deficiency in the global stiffness matrix. Moreover, it is proven that the set of linearly dependent equations is constituted by the inter-element or boundary equilibrium equations related to the lagrangian kinematic variables of two adjacent sides.

In the present paper, SKMs are restrained by a master slave elimination approach, by connecting the kinematic variables related to the linearly dependent equations. The proposed approach reduces the number of kinematic variables and it reduces the global stiffness matrix to a full rank one. Moreover, it preserves verified all the equilibrium conditions, so that numerical solution is actually statically admissible.

Finally, the efficacy of the proposed approach is confirmed by the numerical analysis of one
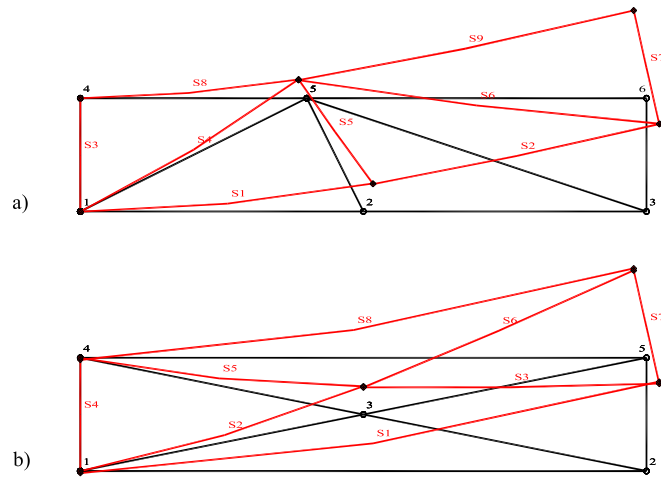
Figure 6: Deformed configuration of: a) mesh 1; b) mesh 2

simple problem, discretized in two different meshes. Eigenvalues analysis confirms that, after application of the restraining approach, no null eigenvalues are produced. The elastostatic numerical analysis response coincides with exact solution for the first load condition whereas, for the second load condition, error in displacement is much lower than in standard finite element solution.

References

[1] Fraeijs de Veubeke B. *Upper and lower bounds in matrix structural analysis.* AGARDograf 1964; 72:165-201.

[2] Fraeijs de Veubeke B. *Displacements and equilibrium models in the finite elements method.* In Stress Analysis, Zienkiewicz OC, Holister GS (eds), Chapter 9. Wiley: London, 1965.

[3] Almeida JPM, Pereira OJBA. *Upper bounds of the error in local quantities using equilibrated and compatible finite element solutions for linear elastic problems.* Computer Methods in Applied Mechanics and Engineering 2006; 195:279-296.

[4] Ladeveze P, Leguillon D. *Error estimate procedure in the finite element method and applications.* SIAM Journal on Numerical Analysis 1983; 20(3):483-509.

[5] Pereira OJBA, Almeida JPM, Maunder EAW. *Adaptive methods for hybrid equilibrium finite element models.* Computer Methods in Applied Mechanics and Engineering 1999; 176:19-39.

[6] J.F. Debongniea, H.G. Zhongb, P. Beckersb. *Dual analysis with general boundary conditions.* Comput. Methods Appl. Mech. Engrg. 122 (1995) 183-192

[7] M. Kempeneers, J.F. Debongnie and P. Beckers. *Pure equilibrium tetrahedral finite elements for global error estimation by dual analysis.* Int. J. Numer. Meth. Engng 2010; 81:513-536

[8] Almeida JPM, Freitas JAT. *An alternative approach to the formulation of hybrid equilibrium finite elements.* Computers and Structures 1991; 40:1043-1047.

[9] Almeida JPM, Pereira OJBA. *A set of hybrid equilibrium finite element models for the analysis of threedimensional solids.* International Journal for Numerical Methods in Engineering 1996; 39:2789-2802.

[10] O. J. B. Almeida Pereira. *Hybrid equilibrium hexahedral elements and super-elements.* Commun. Numer. Meth. Engng 2008; 24:157-165

[11] E.A.W. Maunder, J.P. Moitinho de Almeida. *Hybrid-equilibrium elements with control of spurious kinematic modes.* Computer Assisted Mechanics and Engineering Sciences, 4: 587-605, 1997.

[12] E.A.W. Maunder, J.P. Moitinho de Almeida and A.C.A. Ramsay. *A general formulation of equilibrium macro-elements with control of spurious kinematic modes: the exorcism of an old curse.* International Journal For Numerical Methods In Engineering, Vol 39, 3175-3194 (1996)

[13] E.A.W. Maunder, J.P. Moitinho de Almeida. *The stability of stars of triangular equilibrium plate elements.* Int. J. Numer. Meth. Engng 2009; 77:922-968

[14] E.A.W. Maunder, J.P. Moitinho de Almeida. *A triangular hybrid equilibrium plate element of general degree.* International Journal for Numerical Methods in Engineering 2005; 63:315-350.

[15] RD. Cook *A plane hybrid element with rotational d.o.f. and adjustable stiffness.* International Journal for Numerical Methods in Engineering 1987; 24:14991508.